Physica 141A (1987) 187–210
North-Holland, Amsterdam

PHASE TRANSITIONS IN A CONFINED LATTICE GAS: PREWETTING AND CAPILLARY CONDENSATION

E. BRUNO*, U. MARINI BETTOLO MARCONI and R. EVANS
HH Wills Physics Laboratory, University of Bristol, Tyndall Avenue,
Bristol BS8 1TL, UK

Received 10 March 1986
Revised manuscript received 27 April 1986

The phase equilibria of a lattice gas confined between two parallel walls are investigated in mean-field approximation. Only a finite number of the first-order layering transitions, characteristic of the adsorption isotherms $\theta(\mu)$ for a strongly attractive substrate, survive when the wall-separation H is finite. The sequence is truncated at chemical potential $\mu < \mu_{\mathrm{sat}}$ by the onset of capillary condensation where θ jumps to a large value corresponding to a densely occupied 'liquid' state. Confinement shifts the bulk first-order transition to smaller μ. For weaker wall potentials first-order prewetting transitions, between thick and thin adsorbed films, are observed but these are in competition with capillary condensation. The resulting phase diagram, plotted using the variables $1/H$, μ and T, exhibits a prewetting surface bounded by a line of triple points where thick films, thin films and 'liquid' all coexist, and by a line of prewetting critical points. The factors that influence the extent of this surface are discussed. Results for the lines of coexistence between 'liquid' and 'gas' states and for the location of capillary critical points, where such lines terminate, are presented. These are similar to results obtained from earlier density functional calculations for continuum fluids.

1. Introduction

In this paper we investigate the phase equilibria of a fluid confined by two identical, adsorbing parallel walls separated by a finite distance H, but unbounded in the x–y directions. The fluid, which is in contact with a reservoir at fixed chemical potential μ and temperature T, is represented by a lattice–gas model with nearest-neighbour interactions. Wall–fluid interactions are represented by an external potential $V(z)$ that varies only the z direction, normal to the walls. We are concerned with the influence of confinement on both bulk and surface phase transitions. One of the effects of confining the fluid with attractive walls

---

* Permanent address: Istituto di Fisica Teorica, GNSM-CISM, Universita di Messina, 98100 Messina, Italy.

is to shift the bulk first-order (liquid–gas) transition to smaller values of μ. If bulk coexistence occurs at $\mu = \mu_{\mathrm{sat}}$ for $T < T_c$, the bulk critical temperature, coexistence will occur in the confined system at $\mu < \mu_{\mathrm{sat}}$, with $(\mu_{\mathrm{sat}} - \mu) \propto 1/H$ for large H. This phenomenon, whereby a fluid that is an undersaturated gas in bulk condenses to a 'liquid' in a confined system, is termed capillary condensation (see Evans et al.[1]) and references therein). For sufficiently small H the lines of coexistence of 'gas' and 'liquid' configurations terminate at capillary critical points[1]). These can be viewed as 'shifted' bulk critical points; the shifts arise from the reduction in the net amount of fluid–fluid attraction and from the increase in wall–fluid attraction as H is reduced. Confinement also modifies the various phase diagrams that characterize adsorption at a single substrate. When H is finite the system can no longer exhibit a roughening or a wetting transition since both are associated with the interface between two coexisting bulk phases ($\mu = \mu_{\mathrm{sat}}$). However, finite size does not preclude those surface phase transitions which occur for an undersaturated bulk. These include the first-order layering transitions, in which the amount adsorbed, θ, increases with μ in vertical steps as successive layers of adsorbed gas are deposited on the substrate (e.g. de Oliveira and Griffiths[2]), and the pre-wetting or thick–thin film transition of Cahn[3]) and Ebner and Saam[4]). The latter occurs, for a single wall ($H = \infty$), at temperatures above a first order wetting transition. Suppose such a wetting transition occurs at a point (μ_w, T_w), with $\mu_w = \mu_{\mathrm{sat}}(T_w)$, in the μ–T plane. Then for $T_w \leq T < T_c$ macroscopically thick films of liquid develop at the wall–gas interface when $\mu(T) = \mu_{\mathrm{sat}}(T)$; this is complete wetting ($\theta = \infty$). A line of first order prewetting transitions extends away from (μ_w, T_w) into the single phase 'gas' region – see fig. 1. The coverage θ jumps discontinuously at a prewetting transition so that distinct thick and thin films coexist on the prewetting line. This line terminates in the prewetting critical point $(\mu_{\mathrm{pwc}}, T_{\mathrm{sc}})$, where the films become identical, and lies close to bulk coexistence, i.e. $\mu_{\mathrm{sat}}(T_{\mathrm{sc}}) - \mu_{\mathrm{pwc}}$ is rather small. When H is large but finite we still expect to find prewetting and layering transitions but since these are now in competition with capillary condensation new features can arise.

Our present study was motivated by earlier calculations (Evans and Marini Bettolo Marconi[5]) based on a simple density-functional treatment of a continuum fluid. Our results suggested that the phase equilibria of a confined fluid could be surprisingly rich, especially in the prewetting region. In particular we found a prewetting surface in the space defined by variables $(1/H, T, \mu)$ that was bounded by a line of triple points, where thick films, thin films, and capillary condensed 'liquid' all coexist, and by a line of prewetting critical points. The extent to which such a feature could be regarded as generic was not clear from this work. Moreover we were unable to obtain detailed numerical results for the prewetting surface since even for very large H prewetting

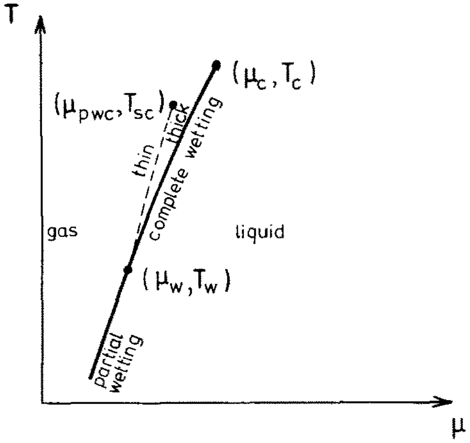

Fig. 1. A schematic μ–T phase diagram for a semi-infinite system ($H = \infty$) exhibiting a first-order wetting transition at (μ_w, T_w). The dashed line is the prewetting line $\mu_{pw}(T)$ where thick and thin films coexist. The solid line is the bulk gas–liquid coexistence line $\mu = \mu_{sat}(T)$. (In the lattice–gas model the bulk coexistence line is vertical: μ_{sat} = constant.)

occurred between metastable thick and thin films, 'liquid' being the stable state of the fluid. The present work was undertaken in an attempt to improve our understanding of the competition between prewetting and capillary condensation. Although somewhat less realistic for fluids than the density functional treatments, the lattice–gas model is more amenable to numerical investigation – at least in the mean-field approximation we employ here. There is a further advantage in that the single-wall ($H = \infty$) version is well studied so we can make use of earlier (Ebner[6,7])) results for this case.

Our paper is arranged as follows: in section 2 we describe the model and the procedure used to determine its (mean-field) solutions. Results of calculations of coverage isotherms for different strengths of wall potential are given in section 3. The relevant phase diagrams are also presented in this section. We conclude, in section 4, by comparing the present results with those from earlier density functional calculations and with a discussion of their possible relevance for computer simulations of adsorption.

2. The model and the method of solution

We consider a lattice gas consisting of N layers confined between two parallel planar walls. The lattice is in contact with a reservoir of particles at temperature T. Each lattice site can be occupied by at most one particle. For simplicity we assume nearest-neighbour interparticle interactions with potential $-\varepsilon$

($\varepsilon > 0$). The total potential felt by a particle in layer j due to wall–particle interactions is

$$V_j = W_j + W_{N+1-j} , \tag{1}$$

where W_j, the potential due to a single wall, is taken to be independent of x and y, i.e. $W_j = W(z_j)$ with z the distance from the wall. The Hamiltonian is then

$$H = -\varepsilon \sum_{\langle jk,\, j'k' \rangle} \sigma_{jk}\sigma_{j'k'} + \sum_{j=1}^{N} V_j \sum_k \sigma_{jk} , \tag{2}$$

where $\sigma_{jk} = 1$ if the kth site in the jth layer is occupied and $\sigma_{jk} = 0$ if it is empty. In the first term of (2) the sum is over all nearest neighbour pairs of sites. The mean-field solution is obtained by minimizing the grand potential functional $\bar{\Omega}$ (see de Oliveira and Griffiths^{2}), where

$$\begin{aligned} \bar{\Omega}/L^2 = \sum_{j=1}^{N} \{ & k_B T(\rho_j \ln \rho_j + (1-\rho_j)\ln(1-\rho_j)) - (\mu - V_j)\rho_j \\ & - \tfrac{1}{2} a\varepsilon\rho_j^2 - b\varepsilon\rho_j\rho_{j+1}(1-\delta_{j,N})\} , \end{aligned} \tag{3}$$

w.r.t. the average occupancies $\{\rho_1, \rho_2, \ldots, \rho_N\}$. Here L^2 is the number of sites in a single layer. Each site has a nearest neighbours in the same layer and b nearest neighbours in an adjacent layer. $\bar{\Omega}$ can be rewritten in a more symmetrical fashion by defining $\rho_0 \equiv \rho_{N+1} \equiv 0$; the last term in (3) is then $-\frac{1}{2} b\varepsilon \sum_{j=1}^{N} \rho_j(\rho_{j-1} + \rho_{j+1})$. The resulting Euler–Lagrange equations are the coupled set

$$m_j = \tanh\left\{ \frac{1}{2k_B T} [\mu' - V_j + \tfrac{1}{2}\varepsilon(a m_j + b m_{j-1} + b m_{j+1})] \right\} , \tag{4}$$

where $j = 1, 2, \ldots, N$, $\mu' = \mu + \frac{1}{2}\varepsilon(a + 2b)$ and we have found it convenient to define new variables $m_j \equiv 2\rho_j - 1$ ($m_0 = m_{N+1} = -1$). In our calculations we employed the same single wall potentials as Ebner^{6}),

$$W(z) = \alpha \frac{4\pi}{45} \varepsilon_w (n_w \sigma_w^3) \left[\left(\frac{\sigma_w}{z}\right)^9 - \frac{15}{2} \left(\frac{\sigma_w}{z}\right)^3 \right] , \tag{5}$$

with parameters chosen to model argon adsorbed on a solid xenon substrate when the strength parameter $\alpha = 1: \sigma_w = 3.735$ Å, $\varepsilon_w/k_B = 160$ K and $n_w\sigma_w^3 = 0.846$. The h.c.p. lattice was located so that the first layer falls in the minimum of $W(z)$, i.e. at $z_1 = (\frac{2}{5})^{1/6}\sigma_w$, and the nearest-neighbour distance was taken to be $2^{1/6}\sigma$ with $\sigma = 3.405$ Å, the atomic diameter of argon. $\varepsilon/k_B = 120$ K. By varying α one can explore the consequences of increasing or decreasing the strength of the attractive substrate potential relative to the attractive interparticle potential; this is particularly useful where one is attempting to ascertain what phase equilibria might occur.

The bulk lattice gas has a symmetrical coexistence curve $\rho_l(T) = 1 - \rho_g(T)$ with chemical potential $\mu_{sat} = -\varepsilon f/2$, independent of temperature T. Here $f = a + 2b$ is the coordination number of the lattice. In mean field approximation the occupancy of the 'gas' phase, $\rho_g(T)$, satisfies

$$(4\rho_g - 2)(\ln[\rho_g/(1-\rho_g)])^{-1} = T/T_c \tag{6}$$

and the bulk critical point is given by $\rho_c = \frac{1}{2}$ and $k_B T_c = \varepsilon f/4$. Thus $\mu_{sat} = \mu_c = -2k_B T_c$. For the h.c.p. structure $a = 6$, $b = 3$ and $f = 12$ so that $k_B T_c = 3\varepsilon$.

Eqs. (4) were solved numerically using an iterative procedure. An algorithm of Ng[8]) was employed to obtain faster convergence. Provided one is not too close to a critical point or to the limit of metastability the procedure is very efficient and often convergence is obtained after 5–10 iterations. For a given μ, T and N it is often possible to find several solutions corresponding to various minima of $\bar{\Omega}$. The solution with the lowest value of $\bar{\Omega}$ gives the equilibrium occupancy profile ρ_j; the others can be identified with distinct metastable states. When two distinct solutions have equal $\bar{\Omega}$ they coexist.

We restrict our consideration to $T < T_c$ and to states for which $\mu(T) < \mu_{sat}(T)$. The 'fluid' is then a gas in bulk with an occupancy $\rho_b = \rho_b(\mu, T)$. A convenient measure of the coverage or adsorption is

$$\theta = \frac{1}{2} \sum_{j=1}^{N} (\rho_j - \rho_b) \, . \tag{7}$$

In the limit $N \to \infty$ θ reduces to the quantity introduced previously by de Oliveira and Griffiths[2]) for adsorption at a single wall. It is useful to measure the degree of undersaturation of the gas at fixed T in terms of the ratio

$$\mathrm{sat} = \rho_b(\mu)/\rho_g(\mu_{sat}) \, , \tag{8}$$

where $\rho_g(\mu_{sat})$ is the occupancy of the bulk gas at coexistence. (sat = 1 at coexistence).

3. Results of calculations

Calculations were performed for different values of the parameter α. For $\alpha = 3$, corresponding to a strongly attractive wall potential, the coverage isotherms have the same form as those obtained by Ebner[6]) and by de Oliveira and Griffiths[2]) except at large values of sat where condensation to a densely occupied 'liquid' state occurs for finite N. A typical low-temperature isotherm is shown in fig. 2. As sat increases the coverage increases from zero in monolayer steps until sat ~ 0.975 when θ jumps from approximately 7 to 50 layers. For larger sat a sequence of layering transitions, in which the coverage increases by amounts of approximately one layer, occur but these now correspond to transitions between metastable states; the equilibrium configuration is

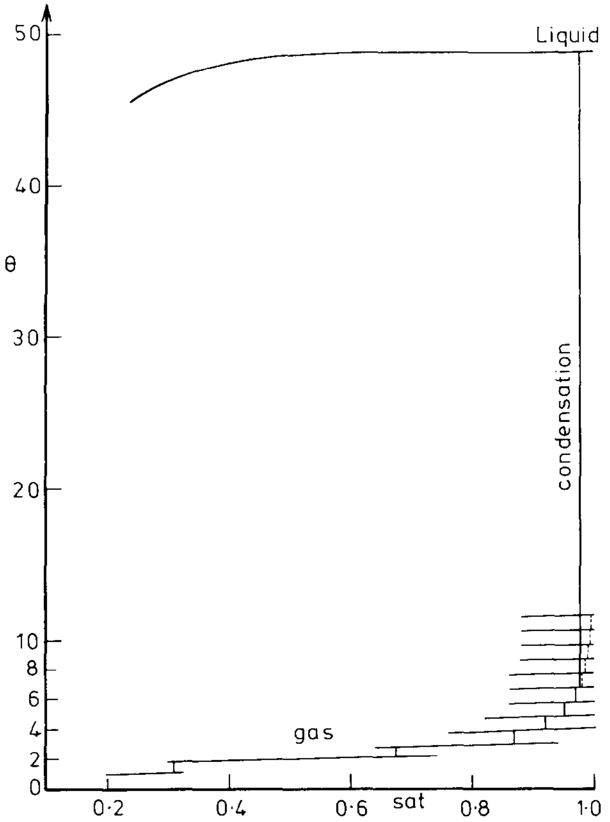

Fig. 2. Coverage isotherm for a strong wall potential ($\alpha = 3$). $T/T_c = 0.45$ and $N = 100$. The short vertical portions represent the jump in θ at first order layering transitions. The dashed vertical lines refer to transitions between states that are metastable w.r.t. the 'liquid' configuration. The sequence of such transitions continues as sat → 1 but is not shown here.

that in which the lattice is densely occupied, i.e. 'liquid'. In the $N=\infty$ case the sequence of layering transitions appears to be infinite for sufficiently attractive wall potentials (de Oliveira and Griffiths[2]), and $\theta \rightarrow \infty$ as sat$\rightarrow 1$ ($\mu \rightarrow \mu_{\text{sat}}$) so that complete wetting occurs for all $0 < T < T_c$. The effect of the finite size is to truncate the sequence of layering transitions. Our result shows that this is not a small effect; although N is very large (100) only 6 stable layering transitions survive before capillary condensation occurs. For smaller N even fewer stable layering transitions survive.

The majority of our calculations were performed for $\alpha = 0.85$. This choice was dictated by the work of Ebner[6]) who investigated the identical model for $N=\infty$. (Ebner mimics the semi-infinite system by requiring his ρ_j to be equal to the bulk gas occupancy ρ_b for $j > 30$.) For this intermediate strength wall potential Ebner finds the transition from partial to complete wetting occurs at $T_w/T_c \approx 0.45$. θ remains finite as $\mu \rightarrow \mu_{\text{sat}}$ for $T < T_w$, whereas it diverges in the same limit for $T_w \leq T < T_c$. The accompanying pre-wetting or thick–thin film transition has its critical point at $T_{sc}/T_c \approx 0.82$. As μ increases along an isotherm with $T_w < T < T_{sc}$, θ first jumps from a value characteristic of a partially filled monolayer to a value corresponding to several layers; this is the signature of the prewetting transition. On further increasing μ θ grows continuously and then increases discontinuously by amounts corresponding to the addition of one layer. The lower the temperature, the larger is the initial discontinuity in θ; the latter becomes infinite at $T = T_w$. For $T > T_{sc}$ there is no prewetting. The purpose of our present calculations was to determine how these phase transitions are modified in a lattice of finite size.

Coverage isotherms are plotted in figs. 3–5. For $N \geq 18$ it is still possible to observe the prewetting transition between stable thick and thin films. This is illustrated in fig. 3 for $T/T_c = 0.70$. In both systems, $N = 100$ and $N = 50$, the transition appears to be identical to that obtained by Ebner[6]). In the larger system we observe a jump of θ on the stable thick film branch and this is the remnant of the first layering transition calculated by Ebner. Condensation to 'liquid' occurs shortly afterwards so that the higher layering transitions found in the $N=\infty$ system become transitions between metastable states for finite N. When N is reduced to 50 (fig. 3b) the thick film is stable over a much smaller range of sat and condensation occurs before the remnant of the first layering transition; this now occurs on the metastable portion. Note that the metastable 'liquid' persists to large undersaturations; we have not attempted to determine accurately the limits of metastability. The coverage θ on the stable 'liquid' branch in the $N = 100$ system is almost exactly twice as large as that in the $N = 50$ system. This follows from the definition (7) and the fact that the ρ_j are nearly constant throughout the lattice on the 'liquid' branch.

On increasing T the discontinuity in θ at the prewetting transition is reduced

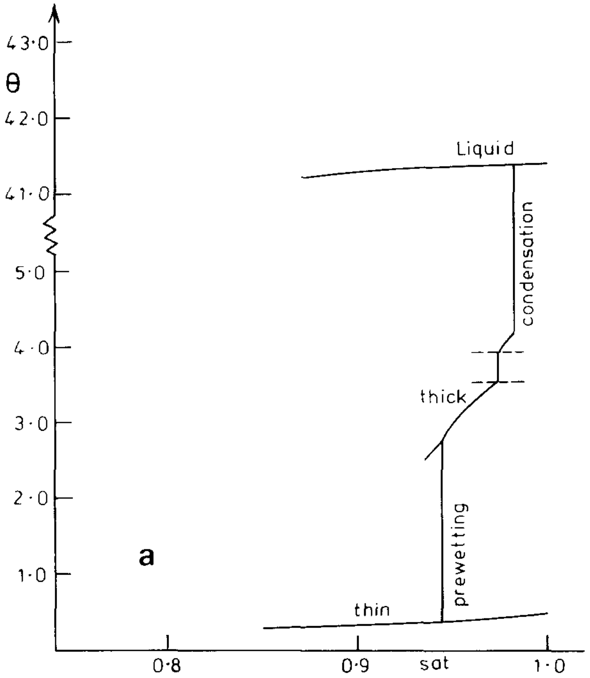

Fig. 3. Coverage isotherms for $\alpha = 0.85$ and $T/T_c = 0.70$, exhibiting both prewetting and capillary condensation. Note the break in the vertical scale; the jump in θ is much larger at condensation. (a) $N = 100$ and (b) $N = 50$. The inset in (b) shows the quantity $\omega \equiv -\Omega/2k_BT_cL^2$ for the various phases. For a given sat the stable phase is that with the lowest grand potential Ω, i.e. largest ω.

until it disappears at $T = T_{sc}$. In fig. 4 we plot θ for $T = 0.825T_c$, which is very slightly above T_{sc}. The 'kink' in θ near sat $= 0.88$ characterizes the prewetting critical point. Note that the 'gas' branch of the isotherm remains the same for different N. Reducing N simply reduces the value of sat at which condensation to the 'liquid' occurs, causing more of the 'gas' branch to become metastable. This is illustrated further in fig. 5 where we plot θ(sat) for $T = 0.9T_c(> T_{sc})$ and for several values of N. For $N > 12$ the 'gas' branch is independent of N and is essentially identical to the $N = \infty$ result. For $4 < N \leqslant 12$ there are differences, especially in the metastable portions. As N is reduced the discontinuity in θ associated with capillary condensation is reduced until, eventually, it disappears near $N = 4$. The isotherm at $N = 4$ is very close to a capillary critical point. For smaller N θ increases monotonically with sat; a full discussion of the definition and genesis of capillary critical points is given by Evans et al.[1]) and later we return to further results for these.

The prewetting coexistence curves, T versus θ, that we calculate for $N = 100$ and $N = 50$ are indistinguishable from that given in fig. 5 of Ebner[6]). What emerges in our present work is the competition between prewetting and

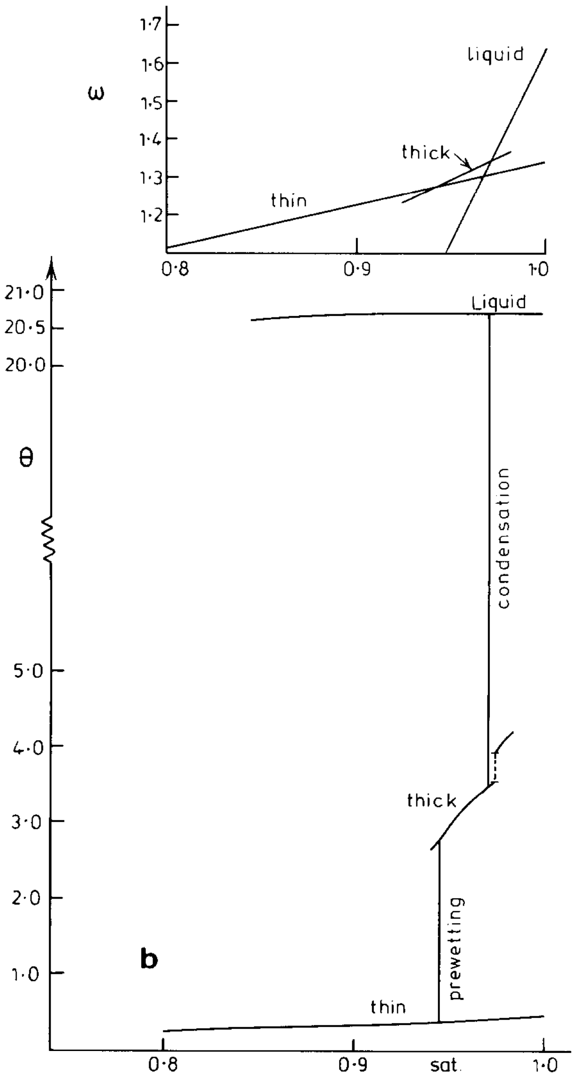

Fig. 3 (continued).

capillary condensation. Both are first-order transitions. The location (measured by sat) of the former is quite insensitive to N, at fixed T, whereas the location of the latter depends strongly on N. Following our earlier work we plot, in fig. 6, our results in terms of three variables: $1/N$, T and sat. The prewetting surface (shaded) is bounded in the $1/N = 0$ plane by the normal prewetting line AB of the semi-infinite system and by a line of surface critical points BC. Since the surface critical temperature T_{sc} is not significantly affected by the size of

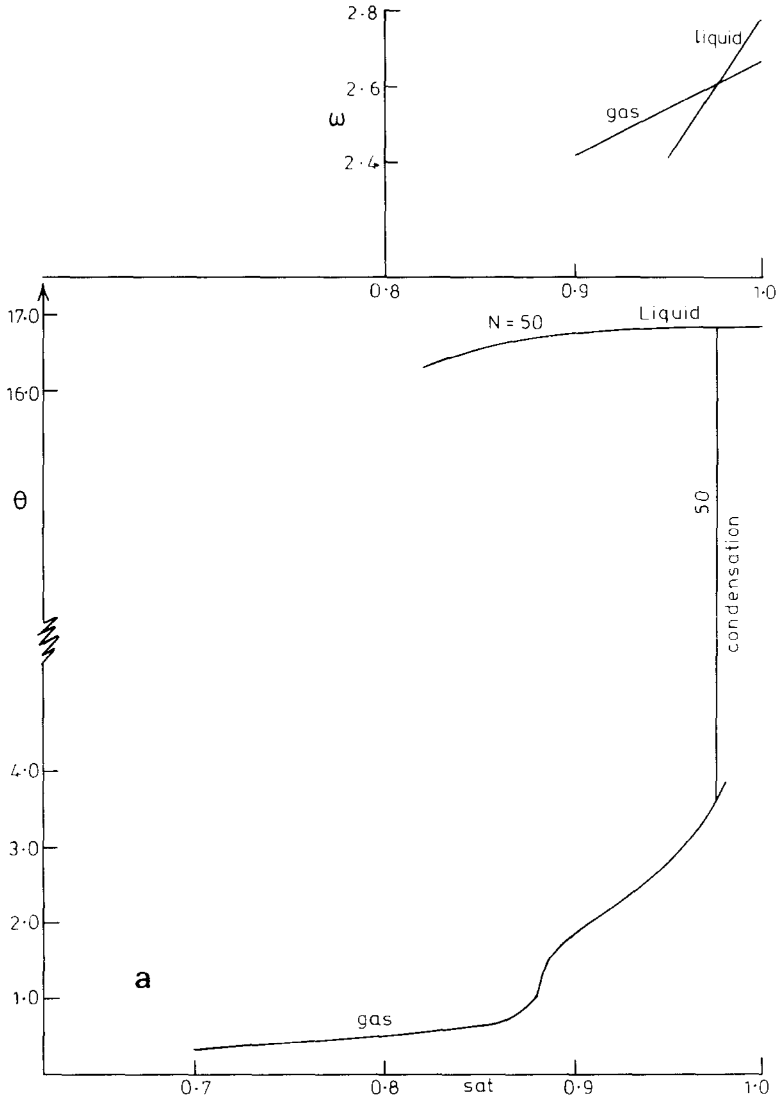

Fig. 4. Coverage isotherms for $\alpha = 0.85$ and $T/T_c = 0.825$, close to the prewetting critical point T_{sc}. (a) $N = 50$. The inset shows ω for 'liquid' and 'gas' solutions near condensation. (b) $N = 18$ and $N = 32$. The 'gas' branch is the same for both N.

the lattice this surface is almost vertical. It intersects the surface formed by the lines of capillary condensation (dashed) in a line of triple points CA. To the right of the prewetting surface ABC (sat→1) and inside the condensation surface 'gas' configurations with thick films are stable, while to the left of ABC (smaller sat) thin films are stable. At a triple point three distinct fluid phases

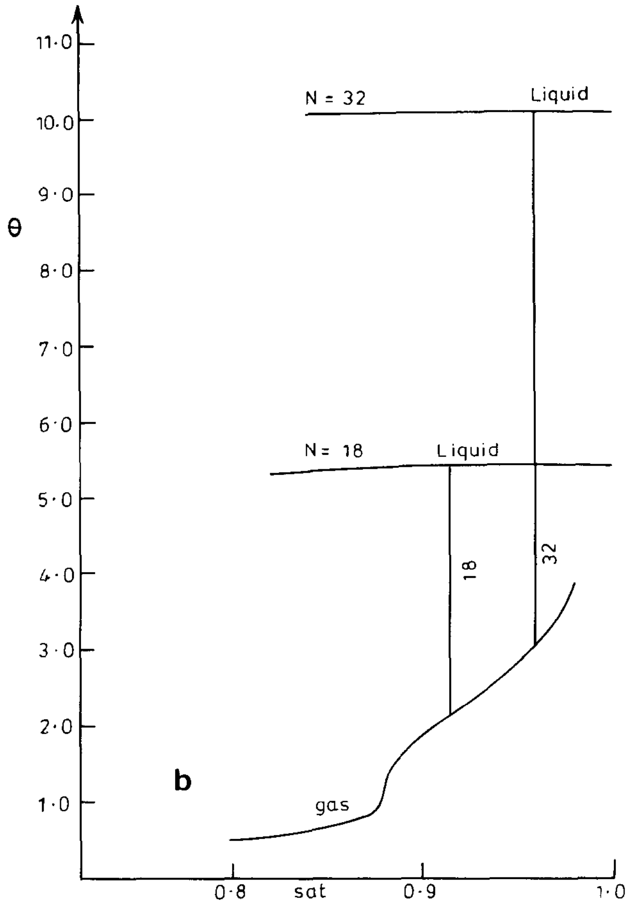

Fig. 4 (continued).

have equal grand potential and coexist; two of the phases are 'gas' with thick and thin films, respectively, and the other is the condensed 'liquid'. Examples of the occupancy profiles ρ_j for two triple point states (marked with open circles in fig. 6) are shown in fig. 7. As T is reduced towards T_w the prewetting surface shrinks to zero; prewetting occurs closer to saturation, driving the triple point line to smaller values of $1/N$. For a maximum lattice size N one can only observe that portion of the prewetting surface that lies above its intersection with the horizontal plane $1/N = \text{constant}$*. The critical end point C corresponds to $N \approx 14$. Note that the lines of capillary condensation continue to

---

* For very small $1/N$ and sat→1 layering transitions can occur. We have not attempted to incorporate these into fig. 6.

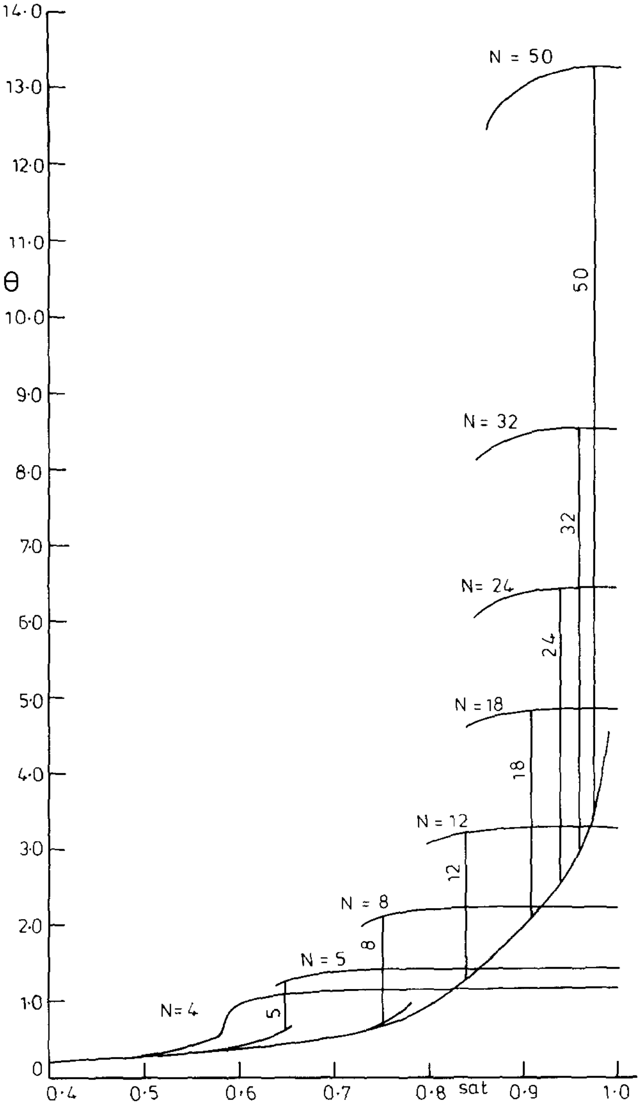

Fig. 5. Coverage isotherms for $\alpha = 0.85$ and $T/T_c = 0.90$ and various N. The vertical portions represent the jump in θ at condensation. The isotherm for $N = 4$ is slightly supercritical.

larger values of $1/N$ and smaller values of sat, terminating eventually in capillary critical points; this is shown explicitly for $T/T_c = 0.9$. The resulting line of critical points $T_c(N)$, curve (a) in fig. 6, terminates at the bulk critical temperature $T_c(\infty) \equiv T_c$ and at $T_c(1) = \frac{1}{2}T_c$ for $N = 1$. The dotted curve (b) is the projection of this line onto the plane $1/N = 0$. In fig. 8 we plot $T_c(N)$ versus N for $\alpha = 0.85$ and for a weaker wall-potential with $\alpha = 0.5$. For $N > 6$

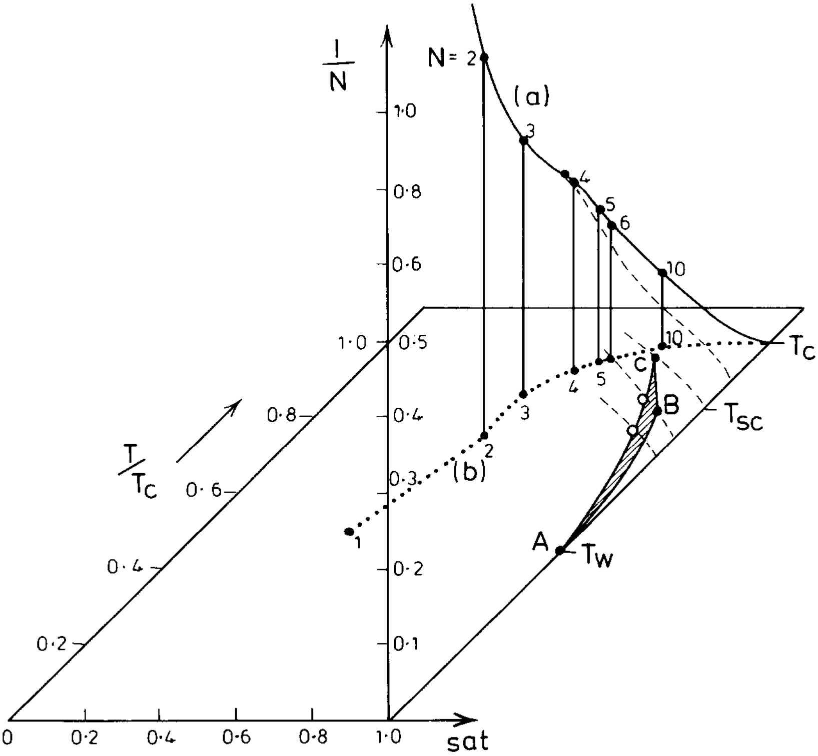

Fig. 6. Phase diagram for $\alpha = 0.85$. Only a portion of the condensation surface is shown (dashed lines). This surface terminates in curve (a), the line of capillary critical points. The prewetting surface ABC (shaded) lies inside the condensation surface and is bounded by the prewetting line AB in the $1/N = 0$ plane, a line of triple points AC and a line of prewetting critical points BC. Other features are explained in the text.

the critical temperatures appear to be insensitive to the choice of α. The log–log plot in the inset shows that $\Delta T \equiv (T_c - T_c(N))/T_c$ decreases as N^{-x}, with $x \sim 1.7$, for $2 \leqslant N \leqslant 8$. A slower decrease occurs for $8 \leqslant N \leqslant 12$ but then a more rapid decay ensues for larger N corresponding to $x > 2$. We should note, however, that for the larger values of N $T_c(N)$ lies very close to T_c so it is difficult in numerical work to determine precisely where the discontinuity in the coverage isotherm disappears. Hence there are considerable inaccuracies in our estimates of $\ln(\Delta T)$ for larger N. Our results do not extend to sufficiently large N to test the prediction of Nakanishi and Fisher[9]), based on scaling arguments for an Ising model with short-ranged (contact) wall-potentials, that $\Delta T \sim N^{-1/\nu}$ as $N \to \infty$. Here ν is the correlation length exponent so that in mean-field approximation $\Delta T \sim N^{-2}$. Nakanishi and Fisher's own numerical results appear to support this prediction.

Also shown in fig. 8 are the results for $T_c(N)$ obtained from a simple slab

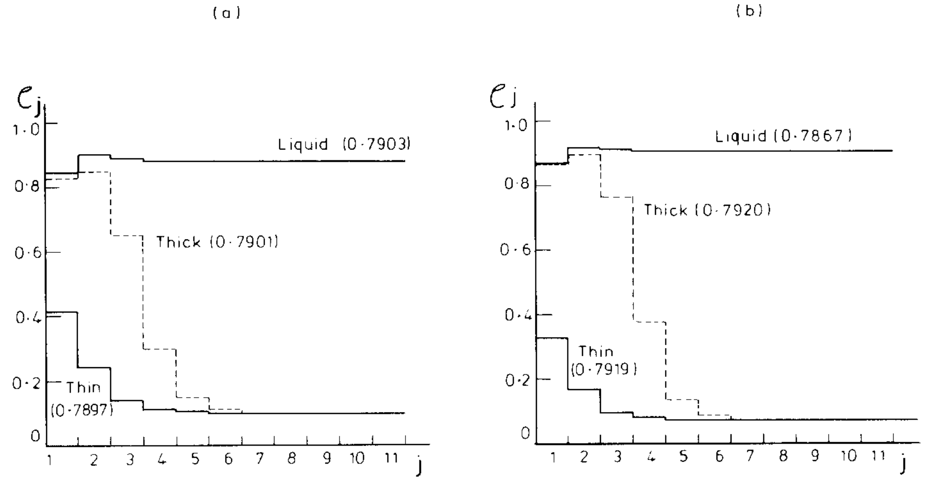

Fig. 7. Occupancy profiles ρ_j for two triple point states. (a) $\alpha = 0.85$, $T/T_c = 0.75$, sat $= 0.920$ and $N = 21$. (b) $\alpha = 0.85$, $T/T_c = 0.70$, sat $= 0.941$ and $N = 29$. Only the portion of each profile near a single wall is shown. The numbers in brackets refer to the reduced grand potential ω of the appropriate phase.

approximation. We digress a little to describe this. By choosing simple parametrized forms for the occupancy profile ρ_j explicit expressions for the grand potential $\bar{\Omega}$ can be derived that can then be minimized w.r.t. the appropriate parameters to obtain equilibrium profiles. The crudest parametrization sets $\rho_j = \bar{\rho}$ for $j = 1, 2, \dots, N$, i.e. the profile is taken to be constant throughout the lattice. From (3) it follows that

$$\frac{\bar{\Omega}(\bar{\rho})}{L^2 N} = k_B T(\bar{\rho}\ln\bar{\rho} + (1-\bar{\rho})\ln(1-\bar{\rho})) - \frac{1}{2} f_N \varepsilon \bar{\rho}^2 - \mu'_N \bar{\rho}\,, \tag{9}$$

where $f_N = a + 2b(1 - 1/N) = f - 2b/N$, is an effective coordination number and $\mu'_N = \mu - \bar{V}_N$ is an effective chemical potential, with $\bar{V}_N \equiv N^{-1}\sum_{j=1}^{N} V_j$, the mean wall–fluid potential. Eq. (9) has the same form as the grand potential of a *homogeneous* lattice gas with occupancy $\bar{\rho}$, but with 'shifted' chemical potential and coordination number. Thus, within this parametrization the phase equilibria of the confined fluid can be obtained directly from that of the bulk fluid. The occupancy of the confined fluid at its critical point, where confined 'liquid' and 'gas' solutions become identical, is

$$\bar{\rho}_c(N) = \rho_c = \tfrac{1}{2}\,, \tag{10a}$$

while

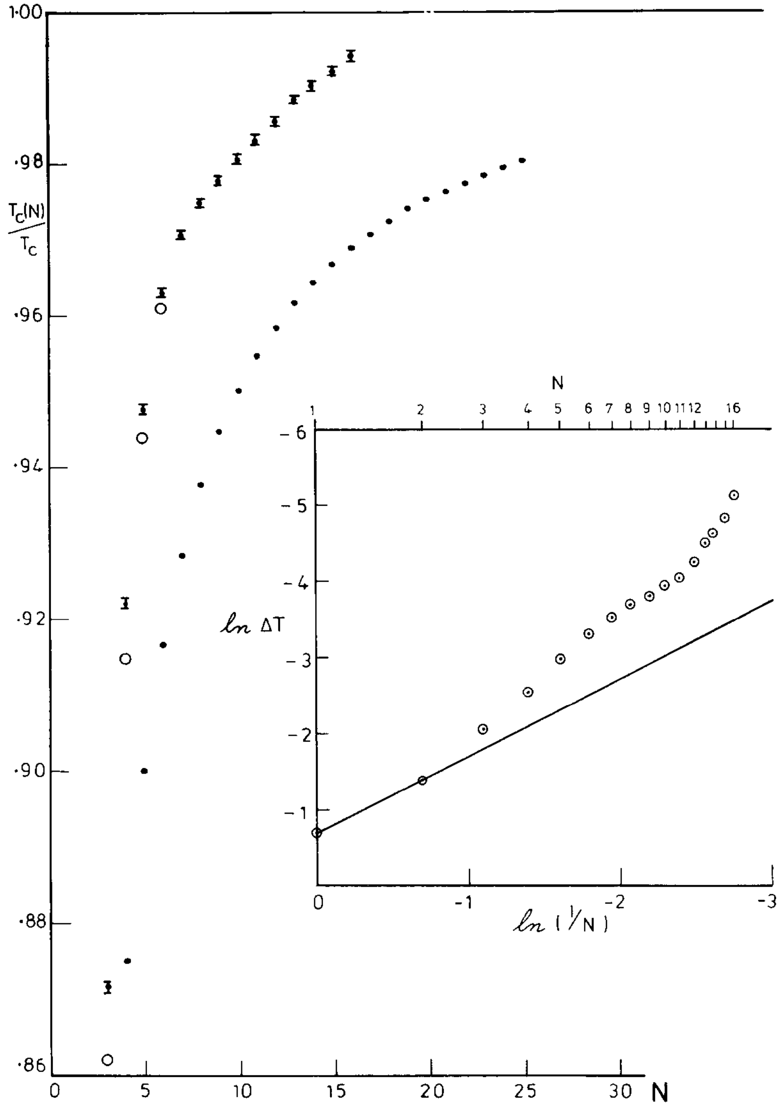

Fig. 8. Capillary critical temperatures $T_c(N)$. The circles ○ correspond to $\alpha = 0.5$ and the points with error bars to $\alpha = 0.85$. The dots are the results from the slab approximation: $T_c(N)/T_c = (1 - 1/2N)$. The results for $\alpha = 0.85$ are plotted on a logarithmic scale in the inset; the straight line corresponds to the slab approximation.

$$k_B T_c(N) = \frac{\varepsilon f_N}{4} = k_B T_c\left(1 - \frac{2b}{fN}\right). \tag{10b}$$

Thus the capillary critical density $\bar{\rho}_c(N)$ and temperature $T_c(N)$ are independent of $\bar{V}_N$ in this approximation. The corresponding chemical potential is

$\mu_c'(N) = -\varepsilon f_N/2 = -2k_B T_c(N)$, from which it follows that

$$\mu_c(N) - \mu_c = \bar{V}_N + \frac{4b}{fN} k_B T_c \,, \tag{10c}$$

where $\mu_c \equiv \mu_c(\infty)$. The dotted curve in fig. 8 denotes the results of (10b) for h.c.p., i.e. $T_c(N)/T_c = (1 - 1/2N)$ or $\Delta T = 1/2N$. Evidently the slab approximation does provide some insight into what factors determine the locus of critical points. $N = 1$ is a special case since this corresponds to a two-dimensional lattice gas in a constant external potential V_1. The latter simply shifts the chemical potential so that coexistence occurs at $\mu = \mu_{co}(1) = V_1 - \varepsilon f_1/2$, where $f_1 = a$, is the coordination number of the two-dimensional lattice. The critical temperature $T_c(1)$ is that of the two-dimensional lattice and $\mu_c(1) = \mu_{co}(1)$. Since the slab approximation is consistent with this argument (10b) yields the correct mean-field result for $N = 1: T_c(1) = \frac{1}{2} T_c$. For $N = 2$, $\rho_1 = \rho_2$ and the slab approximation again yields the correct mean field result $T_c(2) = \frac{3}{4} T_c$. However, at large N, where $T_c(N) \rightarrow T_c$, the approximation $\rho_j = \bar{\rho}$ for all j seems to be completely inadequate and the results agree poorly with those of the full calculation.

It is instructive to enquire if the same approximation can account for capillary condensation. Within this scheme coexistence of the confined 'liquid' and 'gas' configurations, characterized by distinct occupancies $\bar{\rho}_l(N)$ and $\bar{\rho}_g(N)$, is determined by (6) with ρ_g replaced by $\bar{\rho}_g$ and T_c replaced by $T_c(N)$. Coexistence occurs when $\mu_N' = -2k_B T_c(N)$, i.e. at a chemical potential $\mu_{co}(N)$ which is independent of T and which satisfies

$$\mu_{co}(N) - \mu_{sat} = \mu_c(N) - \mu_c = \bar{V}_N + \frac{4b}{fN} k_B T_c \,. \tag{11}$$

(The last step follows from (10c).) In fig. 9 we plot $\Delta\mu_{co} \equiv (\mu_{sat} - \mu_{co}(N))$ against N for $T/T_c = 0.75$ and $\alpha = 0.85$. The condensation line predicted by (11) is in qualitative agreement with the results of the full calculation but overestimates $\Delta\mu_{co}$. Also plotted in fig. 9 are the results obtained from the Kelvin equation for capillary condensation. For sufficiently large N and sufficiently small $(\mu_{sat} - \mu)$ the grand potential of a 'gas' configuration, Ω_g/L^2, can be approximated by $-pN + 2\gamma_{wg}$, where p is the pressure of the bulk 'gas' at chemical potential μ and γ_{wg} is the (single) wall–gas interfacial tension. The latter is defined* as the surface excess grand potential γ evaluated at $\mu = \mu_{sat}$ and $N = \infty$. The corresponding quantity for a 'liquid' configuration under the same conditions, is $\Omega_l/L^2 \approx -p_l^{\dagger} N + 2\gamma_{wl}$, where $p_l^{\dagger}$ is the pressure of the metastable bulk liquid at the same value of μ and γ_{wl} is the wall–liquid

---

[*] Note that the pressure p and the excess grand potential $\gamma = \lim_{N\to\infty}(\Omega/L^2 + pN)$ both acquire the dimensions of energy in this convention.

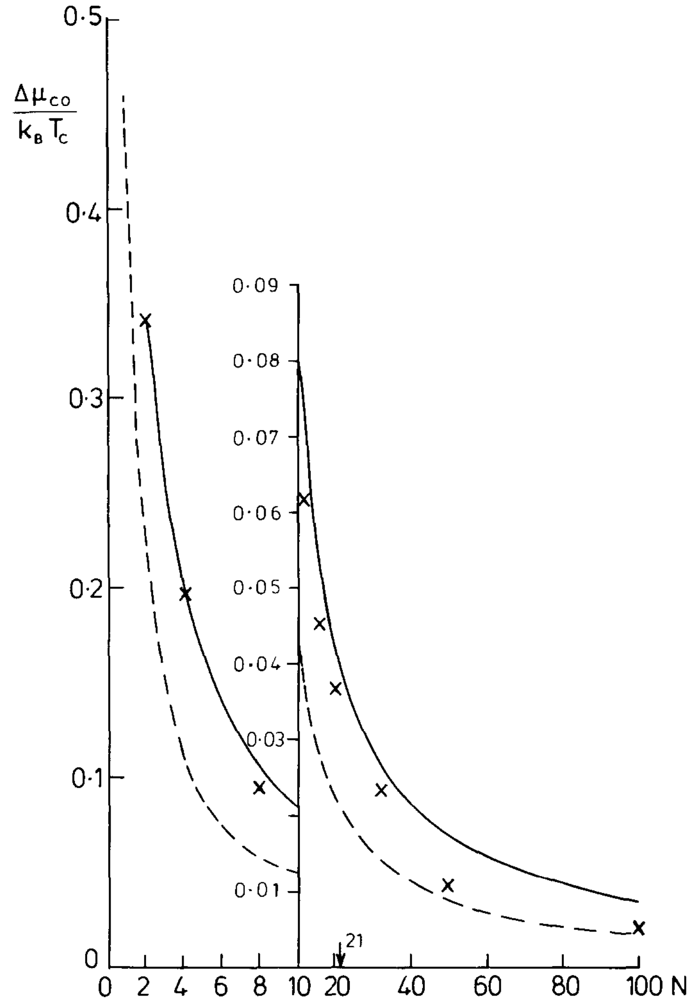

Fig. 9. Capillary coexistence ($\Delta\mu_{co}$, N) diagram for $\alpha = 0.85$ and $T/T_c = 0.75$, a complete wetting situation. The crosses are the results of the full calculations, the solid curve is the slab approximation (11) and the dashed curve is the result of the Kelvin equation (12). The condensation line ends in a capillary critical point at $N = 2$, i.e. $T = T_c(2)$. For $T > T_c(2)$ there is no condensation for $N = 2$. For $T_c(2) > T > T_c(1) = T_c/2$ condensation occurs for $N = 2$ but not for $N = 1$. Note the change in scales at $N = 10$. For $N > 21$ condensation occurs after the prewetting transition – see text.

interfacial tension. Coexistence of 'liquid' and 'gas' occurs when $\Omega_l = \Omega_g$, or when the pressure satisfies

$$p - p_l^{\dagger} = 2(\gamma_{wg} - \gamma_{wl})/N .$$

Expanding both pressures about p_{sat}, truncating at first-order in $\mu - \mu_{sat}$, and using the Gibbs–Duhem relation, we find condensation occurs when

$$\begin{aligned}\Delta\mu_{\mathrm{co}} = \mu_{\mathrm{sat}} - \mu_{\mathrm{co}}(N) &= 2(\gamma_{\mathrm{wg}} - \gamma_{\mathrm{wl}})/N(\rho_{\mathrm{l}} - \rho_{\mathrm{g}}) \\ &= 2\gamma_{\mathrm{lg}} \cos\Theta/N(\rho_{\mathrm{l}} - \rho_{\mathrm{g}}) \,, \end{aligned} \tag{12}$$

where we have used Young's equation, $\gamma_{\mathrm{wg}} = \gamma_{\mathrm{wl}} + \gamma_{\mathrm{lg}} \cos\Theta$, to introduce the contact angle Θ for the single planar wall. Eq. (12) is a version of the Kelvin equation; it is strictly valid in the limit $N \to \infty$. Further details of its derivation and discussion of its limitations for continuum fluids are given in our earlier papers[1,10]). The interfacial tensions γ_{wg} and γ_{wl} were calculated by setting $N = 100$ so that interference effects between the two walls were negligible. From fig. 9 it is clear that eq. (12) underestimates $\Delta\mu_{\mathrm{co}}$. This is consistent with earlier results (Evans et al.[1,10,11])) for a complete wetting situation ($\Theta = 0$); the Kelvin equation usually overestimates the condensation pressure. One might expect that the presence of wetting films on the walls would always tend to raise $\Delta\mu_{\mathrm{co}}$ above the Kelvin value since the effective wall separation is reduced by a multiple of the thickness of the wetting film[10,11]). Indeed for $T = 0.9T_{\mathrm{c}} > T_{\mathrm{sc}}$ we find that the Kelvin equation underestimates $\Delta\mu_{\mathrm{co}}$ by 40% for $N = 50$ and by much larger amounts for smaller N. For $T = 0.75T_{\mathrm{c}} < T_{\mathrm{sc}}$ the situation is somewhat more complex. Prewetting occurs as a transition between stable thin and thick films for $N \gtrsim 21$. Thus for $N > 21$ the condensation is of the type found in fig. 3, i.e. from a thick film to a 'liquid'. Under these circumstances it is appropriate to approximate the interfacial contribution to Ω_{g}/L^2 by $2\gamma_{\mathrm{wg}}$, taking $\gamma_{\mathrm{wg}} = \gamma_{\mathrm{wl}} + \gamma_{\mathrm{lg}}$. For $N < 21$, however, condensation occurs from the thin film to 'liquid' and it is not appropriate to make this approximation. One should employ rather the grand potential corresponding to the thin film. This procedure leads to larger values of $\Delta\mu_{\mathrm{co}}$ but these remain below the results of the full calculations.

In a partial wetting situation ($\Theta > 0$) corresponding to $T < T_{\mathrm{w}}$, the Kelvin equation for continuum fluids was found (Evans et al.[1,11])) to remain accurate down to wall separations of about 10 molecular diameters. Here we find equivalent conclusions for the lattice gas. As an example we plot in fig. 10 $\Delta\mu_{\mathrm{co}}$ versus N for $T/T_{\mathrm{c}} = 0.75$, the same temperature as fig. 9, but for a weaker wall-potential with $\alpha = 0.70$. The contact angle Θ is now about 44° and (12) provides an accurate fit to the numerical results for $N \gtrsim 4$. The slab approximation (11) gives an equally good fit and has the extra merit of yielding the correct mean-field critical point which is at $N = 2$ for this particular temperature.

Finally, we consider in fig. 11 $\Delta\mu_{\mathrm{co}}$ versus N for $\alpha = 0.70$ and a temperature $T = 0.35T_{\mathrm{c}}$, below the two-dimensional critical temperature $T_{\mathrm{c}}(1) = \frac{1}{2}T_{\mathrm{c}}$. The Kelvin equation is very accurate for $N \gtrsim 5$ and the slab approximation (11)

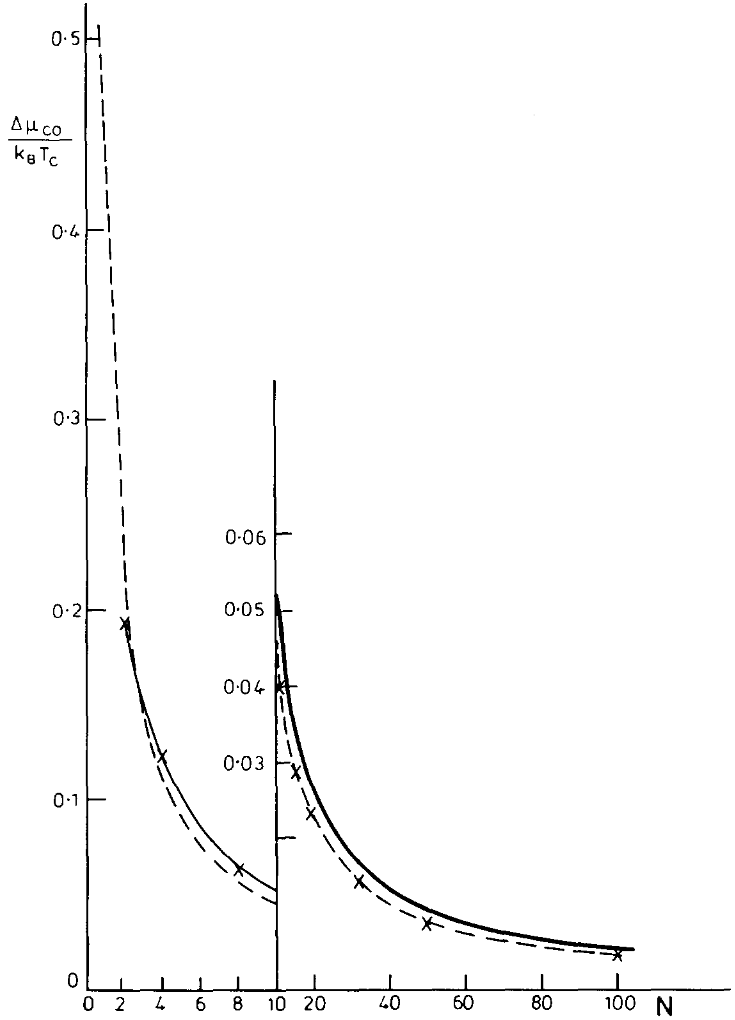

Fig. 10. As in fig. 9 but now for $\alpha = 0.70$ and $T/T_c = 0.75$, a partial wetting situation.

gives an excellent fit to the numerical results for *all* N. Condensation now occurs in all cases, even for $N = 1$. The striking feature is the decrease in $\Delta\mu_{co}$ between $N = 2$ and $N = 1$. This is not an artefact of the slab approximation since eq. (11) yields the correct (mean-field) results for both these cases. For the parameters of our model $V_1 = \bar{V}_1 = -1.66\alpha k_B T_c$ and $\bar{V}_2 = -0.99\alpha k_B T_c$ and (11) implies that for $\alpha > 0.74$, $\mu_{co}(1) < \mu_{co}(2)$, i.e. $\Delta\mu_{co}$ increases monotonically with decreasing N. However, for weaker wall-potentials $\alpha < 0.74$, (11) predicts $\mu_{co}(1) > \mu_{co}(2)$ and we find the behaviour shown in fig. 11. Moreover for

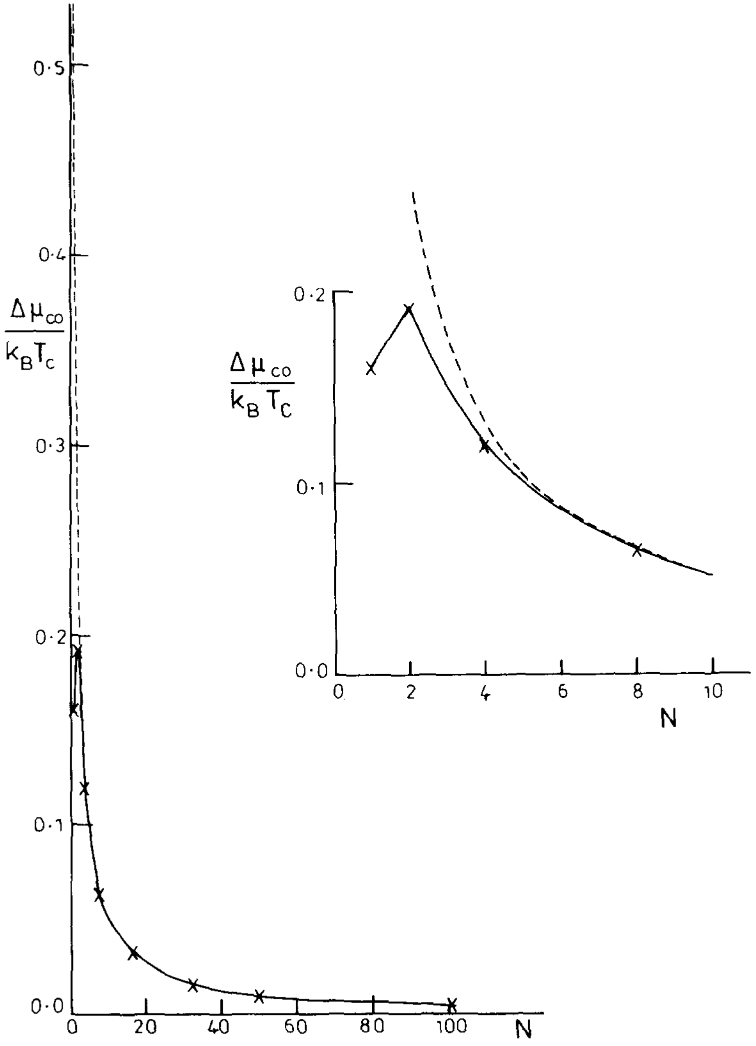

Fig. 11. As in figs. 9 and 10 but now for $\alpha = 0.70$ and $T/T_c = 0.35$. Condensation occurs at $N = 1$; this is not a critical point in this case. The inset shows the results on an expanded scale.

$0.5 \leqslant \alpha \leqslant 0.6$ $\Delta\mu_{co}$ is positive for $N = 2$ but *negative* for $N = 1$ *. Capillary condensation from an undersaturated 'gas' to a 'liquid' occurs for the two layer lattice but capillary evaporation from a supersaturated 'liquid' to a 'gas' occurs for the single layer. For $\alpha \leqslant 0.5$ $\Delta\mu_{co}$ is negative for $N = 2$ and $N = 1$. Eventually one reaches a situation, at sufficiently small $\alpha (< 0.45)$ and T/T_c,

---

* From the *exact* results $\mu_{co}(1) = V_1 - \varepsilon f_1/2$ and $\mu_{co}(\infty) \equiv \mu_{sat} = -\varepsilon f/2$ it follows that, for $N = 1$, $\Delta\mu_{co} = -3\varepsilon - V_1$ in the h.c.p. lattice. Thus, for the present parameters we obtain the exact result $\Delta\mu_{co}(1) = 3\varepsilon(1.66\alpha - 1)$, which changes sign at $\alpha = 0.6$.

where $\Delta\mu_{co}$ is negative for all N. This corresponds to a contact angle $\Theta > \pi/2$ – see (12).

4. Discussion

It is instructive to compare our results with those obtained from the earlier mean-field density functional calculations for continuum fluids. While the gross features of the phase equilibria are the same for the lattice gas model as the continuum fluid there are some important quantitative differences. We focus first on the prewetting surface in fig. 6. It extends to larger values of $1/N(\equiv 1/H)$ than those estimated in ref. 5. In both cases the location of the prewetting line $\Delta\mu_{pw}(H) \equiv (\mu_{sat} - \mu_{pw}(H))$ is insensitive to H and can be approximated by $\Delta\mu_{pw}(\infty)$. Moreover, for large H, $\Delta\mu_{co}$ is given reasonably accurately by the Kelvin equation so that, for fixed T, the separation H_{triple}, at which the condensation surface intersects the prewetting surface, is determined by

$$\Delta\mu_{pw}(\infty) = \Delta\mu_{co}(H) \approx 2\gamma_{lg}/H_{triple}(\rho_l - \rho_g)\,,$$

i.e.

$$H_{triple} \approx 2\gamma_{lg}/(\rho_l - \rho_g)\Delta\mu_{pw}(\infty) \tag{13}$$

with an equivalent result for N_{triple}. In the present case ρ_b/ρ_{sat} is about 0.88 at a prewetting critical point ($T_{sc}/T_c \approx 0.82$), $\Delta\mu_{pwc} \approx 0.046 k_B T_c$ and (13) predicts $N_{triple} \sim 14$, which is close to the calculated value. The density functional results of Evans and Marini Bettolo Marconi[5]) for a Yukawa fluid confined by two hard walls with attractive exponential tails gave $\rho_b/\rho_{sat} \approx 0.95$ for $T_{sc}/T_c = 0.645$ and $\Delta\mu_{pwc} \approx 0.033 k_B T_c$. Thus the prewetting line was much closer to saturation than the present. Since $\gamma_{lg}/k_B T_c$ was much larger than the corresponding quantity for the lattice gas (by a factor of 4, or so) H_{triple} was estimated[5]) to be ~70 molecular diameters at the prewetting critical point. Given that the prewetting line was also much shorter in temperature ($(T_{sc} - T_w)/T_c = 0.065$ rather than the present value of 0.37) it is clear that the prewetting surface for the continuum fluid was very much smaller than that shown in fig. 6 for the lattice gas model. For the fluid it is necessary to go to very large separations, $H > 70$ diameters, before prewetting can be observed between stable thick and thin films, whereas for the present lattice gas prewetting can be observed for $N \gtrsim 15$ when $T \sim T_{sc}$. Will this be true in general? The parameters of the present model were chosen to give a very 'strong' first-order wetting transition at a low temperature. Other choices of parameters and potential functions can produce 'weaker' transitions with shorter prewetting lines. Recent lattice gas calculations by Sen and Ebner[12]) show that the location of the prewetting line depends strongly on the relative ranges of the wall–fluid and fluid–fluid potentials. For many (realistic) choices of potentials they find short lines, $(T_{sc} - T_w)/T_c \lesssim 0.1$, that are close to saturation, $0.01 > \Delta\mu_{pwc}/k_B T_c > 0.001$, in both mean-field and Monte-Carlo treatments. If these estimates are used in (13) they imply very large values for N_{triple} and, hence, extremely small prewetting surfaces, similar to those we described above for the continuum fluid. These observations have repercussions for computer simulations of confined fluids, to which we return later. We note that the profiles displayed in fig. 7 for two states, on, or extremely close to, the triple point line are remarkably similar to the density profiles calculated for a near-triple point state of a continuum fluid confined in a *cylindrical* pore – see fig. 10 of Evans et al.[11]). The decrease of ρ_j near the walls for both the 'liquid' and the thick film appears to be a general feature of such states.

The line of capillary critical points plotted in fig. 8 is similar in shape to that obtained by Evans et al.[1]). If we identify their parameter λ^{-1}, the *common* range of exponential wall–fluid and Yukawa fluid–fluid potentials, with the lattice spacing we find that for large N $T_c(N)/T_c$ decreases less rapidly with decreasing N in the present case. However, comparison of the corresponding slab approximation, eq. (61) of ref. 1, with (10b) indicates the difficulties involved in comparing results from the different models; the former predicts $T_c(H)/T_c \sim 1 - 1/\lambda H$, whereas $T_c(N)/T_c \sim 1 - 1/2N$ for the lattice gas.

Our results for the condensation line $\Delta\mu_{co}(N)$ warrant further comment. As both the Kelvin equation (12) and the slab approximation (11) fail to incorporate the thick wetting films that develop at the walls in a complete wetting situation[1,10,11]) we cannot expect these approximations to provide a quantitative description of condensation for $T > T_w$. In a partial wetting situation, $T < T_w$, both approximations remain reliable down to small values of N, just as was found for continuum fluids[1,11]). The lattice gas model differs from the theory employed in our earlier[1,5,11]) calculations in that it incorporates explicitly two-dimensional liquid–gas condensation when $N = 1$; for $T \geqslant T_c(1)$ there is no condensation for $N = 1$ whereas for $T < T_c(1)$ there is. Such a feature is absent from density functional theories which employ local density approximations for short-ranged (hard-sphere) correlations (see Evans et al.[11])) and can only be incorporated by means of non-local theories (Tarazona et al.[13])). The present prediction that $\Delta\mu_{co}$ may be a non-monotonic function of N (at small N) for weak wall-potentials is rather interesting and one which could be tested by simulation or by the more sophisticated density functional approaches.

Our solutions are strictly mean-field solutions. To what extent could fluctuation corrections modify our conclusions? One obvious defect of the mean-field approximation is its failure to describe a roughening transition. It is well accepted that for strongly attractive wall–fluid potentials the sequence of layering transitions has critical temperatures which approach the roughening temperature T_R as $N \to \infty$ (e.g. Ebner[7])) and that $T_c(1) < T_R < T_c$. Mean-field approximation gives an infinite sequence with critical points approaching the limit T_c as $N \to \infty$, i.e. it implies a roughening temperature equal to the bulk critical temperature. For finite N the sequence is truncated by capillary condensation and there is no roughening. Consequently we can expect the mean-field results to be qualitatively correct. For weaker wall-fluid potentials Ebner[7]) has argued that T_w can be larger than T_R. This implies that layering transitions would not be observed after prewetting as μ is increased towards μ_{sat} and Ebner's Monte Carlo calculations support this view*. By contrast mean-field approximation yields a sequence of layering transitions after prewetting since $T_R = T_c$. When N is finite we once again truncate the sequence but, for sufficiently large N, some layering transitions will remain as shown in fig. 3. It follows that such transitions are probably artefacts of the mean-field approximation. Our general conclusions concerning the existence of a line of triple points and the form of the prewetting surface should remain valid, qualitatively if not quantitatively, in a more rigorous approach. In this context computer simulations could play a valuable role. Our results suggest that for favourable choices of wall–fluid potential, such as the one chosen here, stable prewetting and the accompanying triple point states could be observed in grand canonical Monte Carlo simulations of a confined lattice gas without necessitating prohibitively large wall separations H #. These observations also have relevance for those adsorption experiments that search for prewetting – see Evans and Marini Bettolo Marconi[5]). The competition between prewetting and capillary condensation that is described here could, in principle, be monitored in adsorption measurements performed on an (ideal) porous solid with pores of an appropriate size. Pore geometry and pore connectivity then become relevant however – Evans et al.[11]). For small N, where two-dimensional-like condensation occurs, the effects of fluctuations will become increasingly important and we must expect substantial corrections to the present results, especially for the numerical values of the capillary critical temperatures $T_c(N)$.

---

[*] See also the discussion by Pandit et al.[15]).

[#] Since computer simulations of continuum fluids are usually performed using two identical parallel walls with separations H much less than the values of H_{triple} estimated here, we would *not* expect to see stable prewetting transitions in grand canonical simulations of the type reported by Lane et al.[14]). Indeed prewetting does not appear to have been observed in *any* simulations of continuum fluids.

Acknowledgements

We have benefitted from discussions with P. Tarazona during visits made possible by an Acciones Integradas Grant from the British Council and the Spanish Ministry of Education. We are grateful to A.K. Sen for sending a preprint of his paper. This research was supported by the S.E.R.C. of the U.K. E.B. acknowledges a grant from Dottorato di Ricerche in Fisica of the University of Messina and financial support from GNSM-CISM.

References

1) R. Evans, U. Marini Bettolo Marconi and P. Tarazona, J. Chem. Phys. **84** (1986) 2376. R. Evans and P. Tarazona, Phys. Rev. Lett. **52** (1984) 557.
2) M.J. de Oliveira and R.B. Griffiths, Surf. Sci. **71** (1978) 687.
3) J.W. Cahn, J. Chem. Phys. **66** (1977) 3667.
4) C. Ebner and W.F. Saam, Phys. Rev. Lett. **38** (1977) 1486.
5) R. Evans and U. Marini Bettolo Marconi, Phys. Rev. A **32** (1985) 3817.
6) C. Ebner, Phys. Rev. A **22** (1980) 2776.
7) C. Ebner, Phys. Rev. A **23** (1981) 1925.
8) K-C. Ng, J. Chem. Phys. **61** (1974) 2680.
9) H. Nakanishi and M.E. Fisher, J. Chem. Phys. **78** (1983) 3279.
10) R. Evans and U. Marini Bettolo Marconi, Chem. Phys. Lett. **114** (1985) 415.
11) R. Evans, U. Marini Bettolo Marconi and P. Tarazona, Faraday Symp. Chem. Soc. **20**, to appear.
12) A.K. Sen and C. Ebner, Phys. Rev. B **33** (1986) 5076.
13) P. Tarazona, R. Evans and U. Marini Bettolo Marconi, Molec. Phys., to appear.
14) J.E. Lane, T.H. Spurling, B.C. Freasier, J.W. Perram and E.R. Smith, Phys. Rev. A **20** (1979) 2147.
15) R. Pandit, M. Schick and M. Wortis, Phys. Rev. B **26** (1982) 5112.